Published in final edited form as:
Genes Genet Syst. 2009 October ; 84(5): 327–334.

An insertion of intracisternal A-particle retrotransposon in a novel member of the phosphoglycerate mutase family in the lew allele of mutant mice

Yan Jiao[1,2], **Xiudong Jin**[2], **Jian Yan**[1], **Feng Jiao**[1], **Xinmin Li**[3], **Bruce A. Roe**[4], **Harry W. Jarrett**[5], and **Weikuan Gu**[1]

[(1)]Departments of Orthopaedic Surgery- Campbell Clinic and Pathology, University of Tennessee Health Science Center, Memphis, TN, 38163, USA

[(2)]Mudanjiang Medical College, Mudanjiang, 157011, PR China

[(3)]Clinical Microarray Core, Department of Pathology & Laboratory Medicine, University of California at Los Angeles, 1000 Veteran Ave., Los Angeles, CA, 90095 USA

[(4)]Department of Chemistry and Biochemistry, University of Oklahoma, Norman, OK, 73019 USA

[(5)]Department of Chemistry, University of Texas at San Antonio, San Antonio, TX, 78249, USA

Abstract

Intracisternal A-particle retrotransposons (IAPs) are known, moveable, retrovirus-like elements and are defective in envelope protein synthesis in the mouse genome. Insertion of IAP elements can either interupt or enhance gene function or expression. Using a mouse model called lethal wasting *(lew)*, we recently identified the insertion of an IAP sequence in a gene, *9630033F20Rik*, that contains domains involved in glycolysis. The expression pattern of the *9630033F20Rik* gene between various normal and diseased tissues was determined by semi-quantitative RT-PCR. The effect of the insertion mutation in *9630033F20Rik* on glycolysis in heart, muscle, and brain tissues was further investigated using oligonuleotide microarray analysis. Results indicated that the expression of *9630033F20Rik* is ubiquitous and its signal is relatively higher in heart and brain tissues. The insertion caused the deletion of exon 5 and decreased expression of this gene in all the tissues studied in the *lew* mice. Changes in the expression levels of glycolytic genes mainly occured in muscle tissue, raising a possibility that *9630033F20Rik* may function as one of the transcriptional regulators of glycolytic genes in skeletal muscle. However, considering the fact that a single nucleotide mutation in vesicle-associated membrane protein 1 (VAMP1) has been reported as the causal gene for the *lew* mice, how much of an impact the IAP insertion in the *lew* mouse phenotype has on glycolytic genes compared to the effect from the VAMP1 mutation responsible for the *lew* mouse phenotype should be further investigated.

Keywords

Intracisternal type A particle element; insertion; glycolysis; High-Throughput Screening; Phosphoglycerate mutase

Corresponding author: Weikuan Gu, PhD., University of Tennessee Health Science Center, A302 Coleman Building, 956 Court Avenue, Memphis, TN 38163. Phone: 901-448-2259; Fax: 448-3343; wgu@utmem.edu.

Introduction

Endogenous retroviral elements (ERVs) are retroelements that integrate into a chromosome of a germ cell where they can persist as stable integrated proviruses for multiple generations. ERVs are significant genomic mutagens in mice, causing approximately 10% of all reported spontaneous germ line mutations in laboratory strains (Takabatake et al., 2008; Zhang et al., 2008). Recently, their impact on genome function has brought much attention, especially the intracisternal A-particle retrotransposons (IAPs). IAPs are retrovirus-like elements and are defective in envelope protein synthesis and exist without an extracellular stage. The impact of IAPs on genome evolution and their integration sites have been extensively studied recently (Saito et al., 2008, Zhang et al., 2008). In one particular example, Howard et al. (2008) reported on the activation and transposition of endogenous retroviral elements in hypomethylation induced tumors in mice.

In addition to their own expression and function in the genome, insertion of IAPs in regulatory or normal gene sequences can alter the expression and disrupt the gene's function. Recently, Sun et al. (2008) reported that insertion of an IAP retrotransposon element in the plasma membrane calcium ATPase 2 gene attenuates its expression and produces an ataxic phenotype in joggle mutant mice. Earlier, Zhou et al. (2007) reported that an IAP retrotransposon in the mouse ADAMTS13 gene creates ADAMTS13 variant proteins that are less effective in cleaving von Willebrand factor multimers. Closely relevant to Zhou's short report is the spontaneous muscular dystrophy caused by a retrotransposal insertion in the mouse laminin alpha2 chain gene (Besse et al., 2003).

In this report, we showed presence of an IAP element insertion in the novel gene *9630033F20Rik*, which contains domains involved in glycolysis in a mouse model called lethal wasting (*lew)*. A single nucleotide mutation in vesicle-associated membrane protein 1 (VAMP1) has been reported as the causal gene for the *lew* mice (Nystuen et al., 2007). However, VAMP1 is selectively expressed in the retina and in discrete areas of the brain including the zona incerta and rostral periolivary region and no gross histological abnormalities were observed in those tissues (Nystuen et al., 2007). Our preliminary microarray analysis revealed an inhibition of glycolysis activity, mainly in skeletal muscle. Many muscle wasting related genes were dysregulated in the *lew* mice, suggesting the possibility that insertion of an IAP sequence in *9630033F20Rik* leads to gene expression profile changes. Because *9630033F20Rik* has been ruled out as the candidate gene for the lethal wasting disease in *lew* mice by mapping (Nystuen et al., 2007), the exact impact the IAP insertion has on the *lew* mouse phenotype is not clear.

Materials and Methods

Mice

One pair of heterozygous (*lew/+*) mice were purchased from the Mouse Mutant Stock Resource colonies at The Jackson Laboratory (TJL). A breeding colony was then established by mating them at the University of Tennessee Health Science Center (UTHSC). Experimental animal procedures and mouse husbandry were performed in accordance with the National Institute of Health's Guide for the Care and Use of Laboratory Animals and approved by the UTHSC Institutional Animal Care and Use Committee.

High-Throughput screening of the *lew* Locus

Our aim was to identify a gene that is possibly responsible for the *lew* disease, other than VAMP1. We performed screening using the procedure reported recently (Jiao et al., 2005a, 2005b) around the genomic region of the *lew* locus, which is located on mouse chromosome 6 between D6Mit55 (114.1mbp) and D6Mit111 (113.8 mbp) (Figure 1A). Liver genomic

DNA (gDNA) from +/+, +/*lew*, and homozygous (*lew/lew*) mice were extracted for temperature gradient capillary electrophoresis (TGCE) and sequence analysis. Primer pairs flanking the exons of known and predicted genes (including ESTs) within the *lew* locus were designed with Primer3 software (http://www-genome.wi.mit.edu/cgi-bin/primer/primer3_www.cgi). Primers were located approximately 50 bp from the 5' or 3' of each exon and, in general, produced 300–400 bp amplicons. A TGCE device (SpectruMedix; State College, PA) was used to analyze amplicons from +/+, +/*lew*, and *lew/lew* mouse mixtures. The SpectruMedix system includes a high-throughput capillary electrophoresis instrument capable of analyzing 96 samples every 140 minutes. Heteroduplex analysis was subsequently performed offline using SpectruMedix software. Amplicons from the *lew* mice were sequenced if they differed from the norm.

Total RNA isolation and semi-quantitative RT-PCR

Total RNAs were extracted from 12 different tissues, including skeletal muscle, heart, liver, spleen, thymus, lung, intestine, spine, femur, cerebrum, and cerebellum from female normal and *lew/lew* mice of 13 days of age, with Trizol Reagent (Invitrogen, Carlsbad, CA). The quality of the resultant total RNA was visually determined by observing distinct 28S and 18S ribosomal bands on an agarose gel. The yield and purity of the extracted RNA was quantified by Nano-drop 2000. Samples with a 28S/18S ratio ≥ 1.8 and an A260/A280 ratio of 1.8–2.1 were chosen for this study. Reverse transcription and PCR were conducted using a One-Step RT-PCR kit (Invitrogen). Reactions were performed in a total volume of 50 μl with 8ng/μl of total RNA, dNTP, $MgCl_2$, RNase inhibitor, and primers. First, cDNA synthesis and pre-denaturation were performed in single cycles at 50°C for 40 min and 94°C for 2 min. Next, PCR amplification was performed for 27 cycles: 94°C for 30 sec, 54–58°C for 36 sec, and 72°C for 2 min. The PCR products were analyzed with a 2.0% agarose gel. The quantitative analysis of the PCR products was conducted using Scion Image software (http://rsb.info.nih.gov/nih-image).

DNA sequencing

DNA sequencing was conducted to verify the insertion in the gDNA and cDNA of *9630033F20Rik* following our reported procedure (Jiao et al., 2005a). The same primers in the amplification of DNA fragments from either gDNA or mRNA were also used in the sequencing. Sequencing was conducted two times to verify the result for either gDNA or cDNA.

Microarray analysis

To eliminate some individual variation from later analyses and insure more uniform results, individual heart, skeletal muscle, and cerebrum samples from +/+ (n=3) and *lew/lew* (n=3) mice were pooled into two groups (*Lew* and WT) prior to total RNA isolation. Microarray assay was conducted following the standard Affymetrix (Santa Clara, CA) protocol. Briefly, 8 μg of total RNA from each group was used for cDNA synthesis by the SuperScript Choice System (Invitrogen), followed by cRNA synthesis using the IVT labeling kit (Affymetrix). Affymetrix's mouse genome 430 2.0 arrays were used for cRNA hybridization overnight (16h). Washing, staining, and image scanning were controlled by GCOS 1.4 software (Affymetrix). Raw data was normalized globally with a target signal of 500. Chips with <3 fold resultant scale factor difference were included for data analysis. The dataset was divided into three subsets: cerebrum, heart, and muscle, each with a pair of WT and *Lew* sets. Using GCOS 1.4 software, comparison analyses between WT and *Lew* groups for different tissues were performed based on the Affymetrix change algorithm, in which the Wilcoxon's signed rank test is used to compute p-value of the change call including Increase, Marginal Increase, No Change, Marginal Decrease, or Decrease. In addition, the intensity

log ratio of *Lew* vs. WT was calculated for each probe set based on the Signal Log Ratio Algorithm. To identify differentially expressed genes between different groups, an arbitrary cutoff value of 2.0 fold changes was chosen based on published literature.

Results

Initial gene screening

Our initial screening is for identification of the possible causal gene for the *lew* disease. First, we screened the last exon of every candidate gene within a targeted region (Figure 1A). Our data indicated that there was no sequence difference in these exons between normal and *lew/lew* mice (data not shown). Next, we designed a second pair of primers, flanking the first exon of each gene. From these primers we again did not detect any difference between the normal and the *lew/lew* mice (Data not shown). Finally, we designed our third pair of primers, flanking an exon in the middle of each gene. This time, we noticed that a 252 bp DNA fragment, which includes the exon 5 of a novel gene, named *9630033F20Rik*, was not amplified from the *lew/lew* mice (Figure 1B).

After verification of the non-amplification of the exon5-fragment by different PCR conditions and variable concentrations of DNA and primers, we examined all the other exons of *9630033F20Rik* located on Chr 6 between 127905895 – 127927250 bp using specific primers for each exon. We did not find any sequence differences between normal and *lew/lew* mice in these exons.

Detection of an insertion mutation in exon 5 of 9630033F20Rik

To determine whether exon 5 of *9630033F20Rik* can be amplified from other mouse strains, we conducted PCR amplification using DNA from multiple normal strains and a *lew/lew* sample using the same pair of primers that could not amplify exon 5 from *9630033F20Rik*. As expected, all strains of normal mice (C3H/HeJ, C57BL/6J, BALB/cJ, DBA/1J, A/J, PL/J, CAST/Ei/J, and SJL/J) had a DNA fragment of normal size, while the *lew/lew* mouse did not give a DNA fragment (Figure 1C).

To determine the cause of the 252 bp fragment absence, we designed more pairs of primers covering different parts of exon 5 for PCR amplification using DNA samples from *lew* mice. Our assays showed that the primers with no amplification are located in the genome of *lew* mice (data not shown). Thus, although the primers exist in the *lew* mice, the PCR did not produce the expected, or any other sized, DNA fragment

In order to determine whether the non-amplification is due to a large insertion located within exon 5, we conducted PCR amplification again using the same pair of primers that flank exon 5. This time, we used a long range PCR kit that is specifically designed for the amplification of large DNA fragments. As shown in Figure 1D, a much larger DNA fragment was obtained from the *lew/lew* mice.

Determination of the nature of insertion within the 9630033F20Rik gene

In order to determine the insertion sequences within exon 5 of 9630033F20Rik, we purified the DNA fragment of insertion and conducted DNA sequencing of this fragment. Figure 2A shows partial sequences of inserted DNA sequences. By BLAST search, we found that the insertion sequence belongs to the intracisternal type A particle element (IAP) (ACCESSION: AF532996), which resembles a retrovirus sequence. We also noticed a short sequence of exon5, GGTGAA, was repeated with the insertion of IAP.

In order to investigate the consequence(s) of the IAP insertion on the cDNA from 9630033F20Rik, we amplified cDNA from 9630033F20Rik by conducting RT-PCR amplification using RNA from normal and *lew* mice. A pair of primers flanking exon 2 to exon 6 were used in the RT-PCR. The cDNA fragments were purified and sequenced. As shown in Figure 2B, the entire exon 5 of 9630033F20Rik has been left out in the cDNA sequences of *lew* mice. Figure 2C shows the predicted influences of this mutation on *9630033F20Rik* translation. A protein from *lew* mice is 37 amino acids shorter compared to the normal protein.

The effect of the IAP insertion on the expression of 9630033F20Rik in *lew* mice

To determine the expression pattern of *9630033F20Rik* between different tissues in normal and *lew/lew* mice, we conducted semi-quantitative RT-PCR using 12 different tissues. We used a pair of primers (forward: GGGCAGTTTCTGAGCAATGT; reverse: TCCAACAGGGAAAACCTCTG) that covered exon 3 to exon 6 with a size of 394 bps for normal mice. The amplification indicated that the *9630033F20Rik* expression is ubiquitous and its expression level is relatively higher in heart, cerebrum, and muscle tissues (Figure 3A). Compared with the normal mice, all tissues from *lew/lew* mice had lower expression levels (Figure 3B).

The effect of the insertion mutation on glycolytic gene expression in different tissues of *lew* mice

By domain analysis, we noticed that *9630033F20Rik* contains a stretch of overlay domains involved in glycolysis, including a fructose-2, 6-bisphosphatase (GpmB) domain, and a phosphoglycerate mutase (PGAM) 1 (GpmA) domain. So it is quite likely that *9630033F20Rik* is important somehow in glycolysis. To determine the glycolytic gene expression profile in the situation of the *9630033F20Rik* mutation, we performed microarray assay to simultaneously measure all possible changes in glycolytic gene expression as well as other related changes (Table 1). Since muscle mass, cardiac function, and mental performance are three major affected aspects in muscular dystrophies (Emery, 2002), we surveyed the expression patterns of all other glycolytic genes in muscle, heart, and cerebrum tissues from *lew/lew* mice. The results indicated that most of the glycolytic genes, including *Pgam2*, *Eno1*, *Ldh1*, *Pfkl*, *Tpi1*, *Eno3*, *Pgam1*, *Fbp2*, *Pgk1* and *Pkm2*, in diseased muscle tissues were down-regulated, while in heart tissues only several glycolytic genes, such as *Bpgm*, *Pfkl*, *and Pgam1*, were down-regulated. In the cerebrum, no extra gene down-regulation was observed in diseased cerebrum tissues. However, a couple of genes were slightly up-regulated in heart or cerebrum tissues. Consistent with this altered glycolytic gene expression, the global change in muscle tissue was remarkably greater than the other two tissues. Interestingly, the largest expression changes were in the two major muscle wasting related genes *Fbxo32* and *Trim63* (two proteosome ubiquitin transferase E3 enzymes) in heart and skeletal muscle tissues but not in the brain.

Discussion

Our data indicated that there is an IAP insertion in *9630033F20Rik*, which seems to be a novel glycolytic gene. There are two possibilities for the absence of the 252 bp DNA fragment in the *lew* mice: insertion or deletion mutations. An insertion mutation will cause a larger size PCR product, which is not able to be detected using conditions for normal PCR products. In the event of a deletion mutation, the PCR product should at least include the sequence of one primer from the primer pair. Our data clearly demonstrated that there is a large insertion within exon 5 of *9630033F20Rik*. Our data further suggests the possibility that this insertion may lead to the inhibition or reduction of glycolysis. Glycolysis serves two major roles: the conversion of glucose into pyruvate and the generation of carbon

skeletons for biosynthesis. It is a 10-step process taking place in the cytosol. PGAMs are involved in step eight of this process; interconversion of 2- and 3-phosphoglycerate. Fructose-2,6-bisphosphatase serves a key regulatory role for phosphofructokinase-1 and fructose-1,6-bisphosphate and thus determines whether glycolysis or gluconeogenesis occurs. The IAP elements are members of retrovirus-like structures consistently observable in a variety of mouse tumor cells. They have been implicated in a number of gene mutations (Gwynn et al., 1998). Recently, a spontaneous mouse model of muscle wasting, named dy^{Pas}/dy^{Pas}, was identified as a mutant due to an IAP insertion in the *Lama2* gene, encoding for the extracellular matrix laminin α2 subunit (Besse e tal., 2003). The glycolytic process is tightly controlled in response to conditions both inside and outside the cell.

Three types of enzymes including hexokinase, phosphofructokinase, and pyruvate kinase are generally regarded as the major regulators of glycolysis. Interestingly, our data indicated that the transcripts for all of these three enzymes, such as *Hk1*, *Pfkm* and *Pkm2*, were downregulated in the diseased muscle tissues. Moreover, four major high-abundance distal glycolytic genes, i.e. *Pgam2*, *Eno1*, *Eno3*, and *Ldh1*, were significantly down-regulated in the affected muscle. *9630033F20Rik* contains a fructose-2, 6-bisphosphatase domain, which is involved in both the synthesis and degradation of fructose-2, 6-bisphosphate, a major regulatory molecule that controls glycolysis/gluconeogenesis (Rider et al., 2004). Therefore, the mechanisms for decreased expression of many glycolytic genes may, at least partly, be due to an imbalance in fructose-2, 6-bisphosphate. In addition, other studies have shown that some glycolytic enzymes have additional non-glycolytic functions in transcriptional regulation, apoptosis regulation, and cell motility stimulation (Kim and Dang, 2005). In this regard, it is quite possible that *9630033F20Rik* may function through more than one mechanism to alter glycolytic gene expression in mammals.

It is not clear whether the impaired glycolysis expression is relevant to muscle wasting in *lew* mice because VAMP1 has been regarded as the causal gene for the *lew* disease. It is noticed that VAMP1 is expressed in brain and eye tissues (Nystuen et al., 2007). One would expect that the downregulation of many genes in muscle as well as in heart tissues may be due to the IAP insertion in *9630033F20Rik*. However, VAMP1 mutations in brain and eye tissues may also cause the problem in muscle and heart tissues as well. Muscle phosphoglycerate mutase deficiency has previously been identified as a cause of human metabolic myopathy (Dimauro et al., 1981). A recent report indicates that a severe muscle enolase (Eno3) deficiency causes metabolic myopathy (Comi et al., 2001). Since glycolysis serves dual roles in two basic processes: energy metabolism and biosynthesis, the precise role of impaired glycolysis in the development of muscle wasting needs to be investigated further. A prevailing concept in the understanding of molecular mechanisms of muscle wasting is that Fbxo32 and Trim63 play an important role in most kinds of catabolic condition- and aging- related to muscle wasting (Cao et al., 2005). They are E3 ubiquitin-conjugating enzymes which have been found to be expressed at high levels in many animal models of muscle wasting and human patients with muscular atrophy. A recent microarray study validates this opinion using mouse and rat models of muscle wasting (Lecker et al., 2004). In this study, we observed a remarkable increase of their expression in muscle and heart tissues, suggesting that this extends to the new congenital muscular dystrophy.

In summary, we have identified an IAP insertion in a novel gene which potentially functions in the glycolysis pathway. However, further study is needed to confirm both the function of this gene and the impact of the IAP insertion.

Acknowledgments

Support for this work is from Center of Genomics and Bioinformatics (WG) and Center in Connective Tissue Research (WG), at University of Tennessee Health Science Center; Veterans Administration (WG); National Institute of Arthritis and Musculoskeletal and Skin Diseases, National Institutes of Health (R01 AR51190 to WG; AR051440 to HWJ.) and the Muscular Dystrophy Association (grant #3189 to HWJ).

References

Besse S, Allamand V, Vilquin JT, Li Z, Poirier C, Vignier N, Hori H, Guenet JL, Guicheney P. Spontaneous muscular dystrophy caused by a retrotransposal insertion in the mouse laminin alpha2 chain gene. Neuromuscul Disord. 2003; 13:216–22. [PubMed: 12609503]

Cao PR, Kim HJ, Lecker SH. Ubiquitin-protein ligases in muscle wasting. Int J Biochem Cell Biol. 2005; 37:2088–97. [PubMed: 16125112]

Comi GP, Fortunato F, Lucchiari S, Bordoni A, Prelle A, Jann S, Keller A, Ciscato P, Galbiati S, Chiveri L, Torrente Y, Scarlato G, Bresolin N. Beta-enolase deficiency, a new metabolic myopathy of distal glycolysis. Ann Neurol. 2001; 50:202–7. [PubMed: 11506403]

DiMauro S, Miranda AF, Khan S, Gitlin K, Friedman R. Human muscle phosphoglycerate mutase deficiency: newly discovered metabolic myopathy. Science. 1981; 212:1277–9. [PubMed: 6262916]

Emery AE. The muscular dystrophies. Lancet. 2002; 359:687–95. [PubMed: 11879882]

Glass DJ. Signaling pathways that mediate skeletal muscle hypertrophy and atrophy. Nat Cell Biol. 2003; 5:87–90. [PubMed: 12563267]

Gwynn B, Lueders K, Sands MS, Birkenmeier EH. Intracisternal A-particle element transposition into the murine beta-glucuronidase gene correlates with loss of enzyme activity: a new model for beta-glucuronidase deficiency in the C3H mouse. Mol Cell Biol. 1998; 18:6474–81. [PubMed: 9774663]

Howard G, Eiges R, Gaudet F, Jaenisch R, Eden A. Activation and transposition of endogenous retroviral elements in hypomethylation induced tumors in mice. Oncogene. Jan 10; 2008 27(3):404–8. Epub 2007 Jul 9. [PubMed: 17621273]

Jiao Y, Li X, Beamer WG, Yan J, Tong Y, Goldowitz D, Roe B, Gu W. A deletion causing spontaneous fracture identified from a candidate region of mouse Chromosome 14. Mamm Genome. 2005a; 16:20–31. [PubMed: 15674730]

Jiao Y, Yan J, Zhao Y, Donahue LR, Beamer WG, Li X, Roe BA, Ledoux MS, Gu W. Carbonic anhydrase-related protein VIII deficiency is associated with a distinctive lifelong gait disorder in waddles mice. Genetics. 2005b; 171:1239–46. [PubMed: 16118194]

Kim JW, Dang CV. Multifaceted roles of glycolytic enzymes. Trends Biochem Sci. 2005; 30:142–50. [PubMed: 15752986]

Lecker SH, Jagoe RT, Gilbert A, Gomes M, Baracos V, Bailey J, Price SR, Mitch WE, Goldberg AL. Multiple types of skeletal muscle atrophy involve a common program of changes in gene expression. Faseb J. 2004; 18:39–51. [PubMed: 14718385]

Muntoni F, Voit T. The congenital muscular dystrophies in 2004: a century of exciting progress. Neuromuscul Disord. 2004; 14:635–49. [PubMed: 15351421]

Nystuen AM, Schwendinger JK, Sachs AJ, Yang AW, Haider NB. A null mutation in VAMP1/synaptobrevin is associated with neurological defects and prewean mortality in the lethal-wasting mouse mutant. Neurogenetics. Jan; 2007 8(1):1–10. Epub 2006 Nov 11. [PubMed: 17102983]

Rider MH, Bertrand L, Vertommen D, Michels PA, Rousseau GG, Hue L. 6-phosphofructo-2-kinase/fructose-2,6-bisphosphatase: head-to-head with a bifunctional enzyme that controls glycolysis. Biochem J. 2004; 381:561–79. [PubMed: 15170386]

Saito ES, Keng VW, Takeda J, Horie K. Translation from nonautonomous type IAP retrotransposon is a critical determinant of transposition activity: implication for retrotransposon-mediated genome evolution. Genome Res. Jun; 2008 18(6):859–68. Epub 2008 May 2. [PubMed: 18456863]

Sun XY, Chen ZY, Hayashi Y, Kanou Y, Takagishi Y, Oda S, Murata Y. Insertion of an intracisternal A particle retrotransposon element in plasma membrane calcium ATPase 2 gene attenuates its expression and produces an ataxic phenotype in joggle mutant mice. Gene. Mar 31; 2008 411(1–2):94–102. Epub 2008 Jan 26. [PubMed: 18280673]

Takabatake T, Ishihara H, Ohmachi Y, Tanaka I, Nakamura MM, Fujikawa K, Hirouchi T, Kakinuma S, Shimada Y, Oghiso Y, Tanaka K. Microarray-based global mapping of integration sites for the retrotransposon, intracisternal A-particle, in the mouse genome. Nucleic Acids Res. Jun.2008 36(10):e59. Epub 2008 May 1. [PubMed: 18450814]

Zhang Y, Maksakova IA, Gagnier L, van de Lagemaat LN, Mager DL. Genome-wide assessments reveal extremely high levels of polymorphism of two active families of mouse endogenous retroviral elements. PLoS Genet. Feb 29.2008 4(2):e1000007. [PubMed: 18454193]

Zhou W, Bouhassira EE, Tsai HM. An IAP retrotransposon in the mouse ADAMTS13 gene creates ADAMTS13 variant proteins that are less effective in cleaving von Willebrand factor multimers. Blood. Aug 1; 2007 110(3):886–93. Epub 2007 Apr 10. [PubMed: 17426255]

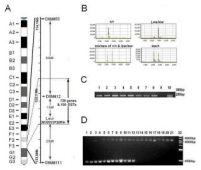

Fig. 1.

Physical localization and identification of IAP insertion of *Lew* gene. **1A**. Location and genetic elements of *lew* locus (9630033F20Rik) previously mapped on murine chromosome 6; **1B.** Sequence analysis of exon 5 amplificant of *Lew* gene from normal (+/+), heterozygous (*lew*/+), homozygous (*lew/lew*) mice and a mixture of +/+ with *lew/lew* samples. The X-axis represents relative size of the PCR products. Y-axis represents relative strength of signal or the amount of the PCR products. **1C.** The PCR amplification products of exon 5 of *Lew* gene from 8 strains of mice and *Lew/Lew* mouse. A pair of primers (forward: GACTAGGTCACCGGCACACT, reverse AGGCCTTTACCATCATGTCG) was designed to flank exon 5 of a *Lew* gene with a size of 252 bps. Samples of lane 1–8 were amplification from C3H/HeJ, C57BL/6J, BALB/cJ, DBA/1J, A/J, PL/J, CAST/Ei/J, SJL/J and lew/lew mice respectively. Lane 10 is DNA marker. ; **1D.** Long-range PCR amplification of *Lew* gene. A pair of primers (forward: GATTAGCTGACAAATGAAATCAAAGA, reverse GTTCTCTGAGGTTCAAGAGACATAAA) was designed to flank exon 5 of a *Lew* gene with a size of 1511 bps. They were used in long-region PCR to amplify a DNA fragment from mice of+/+, *lew*/+ and *lew/lew* genome DNA. Samples of lane 1–4 were amplificants from 4 different normal mice; lanes 5–12 were amplificants from 8 different *lew*/+ mice and lanes 13–21 were amplification products from 9 different individual *lew/lew* mice; lane 22 is DNA marker

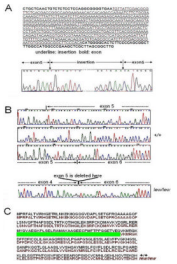

Fig. 2.

Consequences of the IAP insertion mutation. **2A**. Insertion of partial IAP sequence in the DNA sequence of exon 5 of *Lew* gene from *lew*/*lew* mice. **2B**. a stretch of cDNA sequences of *Lew* gene in +/+ and *lew/lew* mice. The deleted section of cDNA sequence in *lew/lew* mice was marked by a dashed arrow. **2C**. Predicted amino acid sequences from *lew/lew* and +/+ mice. Sequences from +/+ and *lew/lew* mice were in black and red, respectively. The deleted predicted sequence in *lew/lew* mice was represented by a green bar.

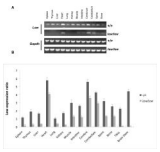

Fig. 3.

Expression pattern of *Lew* in different tissues from normal +/+ and disease *lew/lew* mice by semi-quantitative RT-PCR. A pair of primers (forward:GGGCAGTTTCTGAGCAATGT, reverse: TCCAACAGGGAAAACCTCTG) was designed to cover from exon 3 to exon 6 of *Lew* gene with a size of 394 bps. Three individual 14 days old +/+ and three same age matched three *lew/lew* mice RNA samples from 12 different tissues were used for this experiment and a duplicate well was run for each sample. The figure only shows one sample from each type on the gel image. After electrophoresis (**3A**) and scanning, all PCR product bands were analyzed by using the software Scion Image and relative mRNA expression was estimated by normalization with *Gapdh*. The final ratios were calculated by dividing the relative values of different tissues by the lowest value for lung of normal mice (**3B**).

Table 1

Effect of *Lew* mutation on gene expression in *lew* mice (fold changes)

Gene category	Gene symbol	Muscle	Heart	Cerebrum
Total number of altered genes		2304	1024	257
Glycolysis-associated genes	9630033F20Rik	−2.3	−1.3	−1.9
	Eno1	−2.8	0	0
	Ldh1	−2.1	−1.2	0
	LOC433182	−2	0	0
	Pgam2	−2	0	0
	Pfkl	−1.9	−1.6	0
	Tpi1	−1.9	0	0
	Eno3	−1.7	0	1.7
	Fbp2	−1.7	1.6	0
	Pgam1	−1.7	−1.6	0
	Hk1	−1.6	0	0
	Pfkm	−1.6	0	0
	Pgm1	−1.6	0	0
	Pkm2	−1.6	0	1.2
	Bpgm	−1.5	−3	0
	Pgk1	−1.5	0	0
	Pgm2	−1.5	1.3	0
	Ldh2	0	1.5	1.2
Muscle wasting-associated genes	Fcmd	−1.9	1.3	0
	Fkrp	−1.4	0	0
	Sepn1	−1.6	−1.6	0
	Col6a1	−1.9	−1.4	0
	Col6a2	−2.1	−1.6	0
	Col6a3	−1.9	−1.5	0
	Large	−2.5	−1.6	0
	Fbxo32	29.9	3.5	0
	Trim63	4.9	2.8	0